Atmospheric
Measurement
Techniques

Open Access

Discussions

A broad supersaturation scanning (BS2) approach for rapid measurement of aerosol particle hygroscopicity and cloud condensation nuclei activity

H. Su[1], Y. Cheng[1], N. Ma[2], Z. Wang[1], X. Wang[1], M. Pöhlker[1], B. Nillius[1], A. Wiedensohler[2], and U. Pöschl[1]

[1]Multiphase Chemistry Department, Max Planck Institute for Chemistry, Mainz 55020, Germany
[2]Leibniz-Institute for Tropospheric Research, Leipzig 04318, Germany

Correspondence to: Y. Cheng (yafang.cheng@mpic.de)

Discussion Paper | Discussion Paper | Discussion Paper | Discussion Paper

AMTD

8, 9713–9730, 2015

A broad supersaturation scanning (BS2) CCN counter

H. Su et al.

Title Page

Abstract	Introduction
Conclusions	References
Tables	Figures

⏮ | ⏭

◀ | ▶

Back | Close

Full Screen / Esc

Printer-friendly Version

Interactive Discussion

Abstract

The activation and hygroscopicity of cloud condensation nuclei (CCN) are key to understand aerosol–cloud interactions and their climate impact. It can be measured by scanning the particle size and supersaturation in CCN measurements. The scanning of supersaturation is often time-consuming and limits the temporal resolution and performance of CCN measurements. Here we present a new approach, termed broad supersaturation scanning (BS2) method, in which a range of supersaturation is simultaneously scanned reducing the time interval between different supersaturation scans. The practical applicability of the BS2 approach is demonstrated with nano-CCN measurements of laboratory-generated aerosol particles. Model simulations show that the BS2 approach is also applicable for measuring CCN activation of ambient mixed particles. Due to its fast response and technical simplicity, the BS2 approach may be well suited for long-term measurements. Since hygroscopicity is closely related to the fraction of organics/inorganics in aerosol particles, a BS2-CCN counter can also serve as a complementary sensor for fast detection/estimation of aerosol chemical compositions.

1   Introduction

Aerosol particles serving as cloud condensation nuclei (CCN) influence the cloud formation process and play an important role in regulating the radiative budge of the earth system (Pruppacher and Klett, 1997). The abundance of CCN is one of the key prerequisites for better understanding and assessment of aerosol–cloud interactions and its climate effect. To predict CCN concentrations, knowledge about the aerosol size distribution and CCN activities (hygroscopicity) is required.

The CCN activities can be determined by the size-resolved CCN measurements in which both dry particle diameter (D_d) and supersaturation (S) are scanned. Based on

such measurements, the CCN activity parameter (e.g., κ) can be determined by the corresponding Köhler equation (Köhler, 1936; Petters and Kreidenweis, 2007).

Fast scan of S is important for measurements of ambient CCN with high temporal variability. The DMT (Droplet Measurement Technologies) CCN counter (CCNC) is one of the most commonly used CCNC nowadays (Roberts and Nenes, 2005). The change of S in this type of CCNC can be achieved by changing the thermal-gradient in the activation tube. This approach requires a waiting time of a few minutes to stabilize the newly designated S which largely reduces the time-resolution of S scan. Due to the low time-resolution, CCN activities are normally measured at only a few S to account for the temporal variability of ambient aerosol particles (Gunthe et al., 2011; Rose et al., 2011). To increase the time-resolution of S scan, the Scanning Flow CCN Analysis (SFCA) was developed in which S was continuously adjusted by changing the flow rate in the activation tube (Moore and Nenes, 2009). SFCA makes possible the rapid and continuous measurement of S spectra, with a time resolution of $\sim$ 10–60 s. Fast scan of S has also been achieved for other designs of CCNC in the work of Fukuta and Saxena (1979) and Hudson (1989).

This study presents a new approach, termed broad supersaturation scanning (BS2) methods, which measures the activation of CCN simultaneously over a continuous range of S and reduces the time required for S scan to infinitely small. This enables the fast determination of κ, which is useful for both CCN modeling/prediction and estimation of aerosol chemical compositions (Wang et al., 2015). Besides advances in the time-resolution, BS2-CCNC may be built with simple modifications of existing DMT-CCNC. In addition, both temperature gradient and flow rate are kept constant during the measurements, minimizing the potential problem of aerosol volatilization and technical complexity (Moore and Nenes, 2009).

2 Methodology

2.1 Concept of BS2 approach

For easy understanding, we introduce the BS2 method in comparison with previous designs and applications of DMT-CCNC. Figure 1a shows a typical distribution of supersaturation in the activation tube of DMT-CCNC, denoted as S_{tube}. S_{tube} is a function of r, the radial distance to the centerline of the activation unit. The highest S_{tube} appears in the centerline and drops to 0 near the wall. Note that S_{tube} in the activation tube also has an axial dependence (Roberts and Nenes, 2005), here we simply use S_{tube} to represent the maximum S in the axial direction at a given r.

Figure 1a and b shows regular applications of DMT-CCNC, in which aerosol particles are focused on the centerline by a narrow aerosol inlet and laminar sheath flow. Such application ensures that aerosol particles are exposed to a single S_{tube} at the centerline (Fig. 1b). Then depending on the values of S_{tube} and $S_{aerosol}$ (the critical activation supersaturation of aerosol particles), the activation fraction F_{act} can be either 0 ($S_{aerosol} > S_{tube}$) or 1 ($S_{aerosol} < S_{tube}$).

Figure 1c shows the dependence of F_{act} on $S_{aerosol}$ in a single S scan (i.e., with given S_{tube}). It is clear that the F_{act} value (0 or 1) measured in a single S scan is not sufficient to determine $S_{aerosol}$ (because it corresponds to infinite values of $S_{aerosol}$). To determine the exact $S_{aerosol}$, multiple S scans (i.e., scanning different S_{tube}) are required until F_{act} changes from 0 to 1. The interval of S_{tube} scans determines the uncertainty of $S_{aerosol}$. When the adjustment of S_{tube} is slow, only a few S_{tube} can be scanned leading to a large S_{tube} interval and uncertainties in the derived $S_{aerosol}$. That is why we need a fast S scan approach such as BS2 or SFCA.

In the BS2 approach, we make use of the whole S distribution inside the activation chamber. Instead of being focused at the centerline, the measured aerosol particles are introduced with a wider inlet (or with a high aerosol-to-sheath flow ratio) and distributed in a broad cross-section of the activation tube (Fig. 2). In this case, aerosol particles are exposed to a range of S_{tube} simultaneously. For a population of aerosol particles

with the same S_{aerosol}, the total activation fraction, F_{act}, can be calculated by integrating the activation fraction function $g(x)$ over the cross section of the aerosol flow, i.e., from the center ($r = 0$) to the edge of the aerosol flow,

$$F_{\text{act}} = \frac{2\pi \int_0^r g(S_{\text{aerosol}} - S_{\text{tube}}) r \, dr}{2\pi \int_0^r r \, dr}, \quad \text{in which } g(x) = \begin{cases} 1 & \text{if } x \leq 0 \\ 0 & \text{if } x > 0 \end{cases} \tag{1}$$

5 Figure 2c shows the dependence of F_{act} on S_{aerosol} for a BS2 measurement based on the S_{tube} distribution in Fig. 2b. Such monotonic dependence suggests that S_{aerosol} can be directly determined once F_{act} is measured. For a given S_{tube} profile, we have a fixed F_{act}–S_{aerosol} relation (Fig. 2c), which can be determined with calibration aerosols (Section. 2.2). The upper limit of measurable S_{aerosol} by BS2 equals the maximum S_{tube} on
10 the centerline, while ideally the lower limit can be zero depending on the width of the aerosol flow in relevance to the activation tube (Fig. 2a). For size-resolved measurements, we can calculate the corresponding hygroscopicity parameter κ of aerosols particles from S_{aerosol} and the particle diameter D_{d} by (Petters and Kreidenweis, 2007; Su et al., 2010)

15 $$\kappa \approx \frac{4A^3}{27(\ln(S_{\text{aerosol}}/100\,\% + 1))^2 D_{\text{d}}^3} \quad \text{with } A = \frac{4\sigma_{\text{sol}} M_{\text{w}}}{RT\rho_{\text{w}}} \tag{2}$$

in which σ_{sol} is the surface tension of water, M_{w} is the molar mass of water, R is the gas constant, T is the temperature in Kelvin, and ρ_{w} is the density of liquid water.

2.2 Calibration

For the BS2 calibration, the goal is to determine the monotonic F_{act}–S_{aerosol} relation as
20 shown in Fig. 2c. This can be achieved by performing size-resolved measurements of pure calibration aerosols with known hygroscopic properties, e.g., ammonium sulfate aerosol particles. Each D_{d} corresponds to a specific S_{aerosol} (Eq. 3), and by recording

Title Page

Abstract | Introduction

Conclusions | References

Tables | Figures

|◀ | ▶|

◀ | ▶

Back | Close

Full Screen / Esc

Printer-friendly Version

Interactive Discussion

the corresponding F_{act}, we get the calibration curve of F_{act}–$S_{aerosol}$ relation.

$$S_{aerosol} \approx 100\,\% \cdot \left(\exp\left(\sqrt{\frac{4A^3}{27\kappa D_d^3}} \right) - 1 \right) \qquad (3)$$

2.3 Application

The first step for the BS2 measurement is to select proper S_{max}, the maximum S_{tube} in the centerline of the activation unit. S_{max} should be higher than the highest $S_{aerosol}$ of investigated aerosol particles. Given the range of particle size and κ, S_{max} can be estimated from Eq. (3). An example is given in Fig. S1 in the Supplement to illustrate the relationship between S, κ and D_d. The adjustment of S_{max} can be done by changing the temperature gradient of the tube (Roberts and Nenes, 2005; Rose et al., 2008; Wang et al., 2015).

Once a proper temperature gradient is selected, we can perform size-resolved CCN measurements with BS2 analysis and record the BS2 activation spectra, i.e. the activation fraction F_{act} as a function of the dry particle diameter D_d. Based on the calibration curve (i.e., F_{act}–$S_{aerosol}$ relation), we can calculate the size-resolved $S_{aerosol}$ as well as κ (by Eq. 2). Figure 3 shows the size-resolved F_{act}–κ relation for a S_{tube} profile as given in Fig. 2b.

3 Results and discussion

3.1 Imperfect internally mixed aerosol with a single κ mode

For aerosol particles of the same composition (pure compounds or perfectly internally mixed compounds), its $S_{aerosol}$ and κ values can be readily determined as described in Sect 2.3. Under ambient conditions, however, aerosol particles (even of the same size) often consist of different chemical compositions and hence different κ (Lance et al.,

2007; Su et al., 2010; Gunthe et al., 2011). In this section and Sect 3.2, we will discuss the application of BS2 approach in ambient measurements.

Most CCN and HTDMA (hygroscopicity tandem differential mobility analyser) measurements show that ambient aerosol particles often have a near single lognormally distributed κ mode especially at the clean and background sites (Su et al., 2010). Here we assume that the investigated aerosol particles have a lognormal κ distribution with a geometric mean κ of 0.3. Since the broadening of κ distribution is a major difference between pure and ambient aerosol particles, we take a series of broadening factor, i.e. the geometric standard deviations σ_κ of the κ distribution for further discussion of the BS2 application.

As shown in Fig. 4, for aerosols with a single κ value ($\sigma_\kappa = 1$), we can get the same κ value of 0.3. For aerosols with a broad κ distribution, the retrieved κ depends on F_{act}. When $F_{act} > 0.2$, the retrieved κ is very close to their geometric mean value with a relative difference of $< 5\%$. When $F_{act} < 0.2$, the retrieved κ can be largely biased from the geometric mean. The reason for this is as follows. Since F_{act} shows a monotonic dependence on κ, a κ distribution will in fact result in a F_{act} distribution. Then the influence of high and low F_{act} will largely cancel out leading to a κ close to the geometric mean value. When F_{act} is close to zero, the influence becomes asymmetric (because F_{act} of the less hygroscopic aerosols cannot be smaller than zero). Then the effect of more hygroscopic aerosols dominates the signal resulting in a much higher retrieved κ. In such a case, we may increase the S_{max} to ensure $F_{act} > 0.2$.

3.2 Externally mixed aerosols with two κ modes

At clean and background sites, most CCN and HTDMA measurements show a single κ mode. During biomass burning events, another less hygroscopic mode often appears at size range of $D_d > 100\,nm$ (Rose et al., 2011). In Fig. 5a, we assume that aerosols have two lognormally distributed κ modes with mode κ of 0.3 and 0.01 (Rose et al., 2011). The number fractions of the two modes (denoted as $a_{\kappa_{0.3}}$ and $a_{\kappa_{0.01}}$) are size-

dependent at 100–200 nm size range (Rose et al., 2011),

$$a_{\kappa_{0.01}} = 0.3 \times \log_{10}(D_d/30) \quad \text{and} \quad a_{\kappa_{0.01}} = 1 - a_{\kappa_{0.3}} \tag{4}$$

in which the unit of D_d is nanometer.

Figure 5b shows the modeled result for measurements with a BS2 approach (labeled as "apparent"). The retrieved κ varies from 0.11 to 0.26, which lies between the κ values of the two modes (i.e., 0.01 and 0.3). This is because the measured activation fraction F_{act} is an average of individual modes weighted by their number fraction

$$F_{act} = a_{\kappa_{0.3}} \times F_{act,\kappa_{0.3}} + a_{\kappa_{0.01}} \times F_{act,\kappa_{0.01}} = (1 - a_{\kappa_{0.01}}) \times F_{act,\kappa_{0.3}} + a_{\kappa_{0.01}} \times F_{act,\kappa_{0.01}} \tag{5}$$

The retrieved κ (~ 0.11 to 0.26) follows the change of the geometric mean values (~ 0.11 to 0.18) and represent certain kinds of weighted average of the two κ modes. This result suggests that the BS2-CCNC alone cannot be used to resolve multi-mode structure of κ distribution.

To resolve the dual κ-mode or multiple κ-mode, we need to decouple the mixed information in Eq. (5) and extract the signal of each mode (i.e., $F_{act,\kappa_{0.3}}$ or $F_{act,\kappa_{0.01}}$) by combining BS2-CCNC with other complimentary techniques. The idea here is (1) to use a DMT-CCNC to determine $a_{\kappa_{0.01}}$; and (2) to choose a S_{max} of BS2-CCNC low enough so that $F_{act,\kappa_{0.01}} = 0$. In such a way, we can solve $F_{act,\kappa_{0.3}}$ from Eq. (5) and determine κ of the more hygroscopic mode. In the 100 to 200 nm size range, for example, the two hygroscopic modes aforementioned can be separated by setting S of DMT-CCNC around 0.37 % (Fig. 5a) and set S_{max} and S_{tube} profile of BS-CCNC the same as in Fig. 2b.

Figure 5b shows that we are able to resolve the mean κ of the more hygroscopic mode (labeled as "corrected") with such combination of measurements. κ of the less hygroscopic mode can be resolved with a similar approach, in which we run in parallel a DMT-CCNC with S of 0.37 % and a BS-CCNC with higher S_{max} (~ 1.5 %) and $S_{min} \sim$ 0.37 %. The adjustment of S_{min} can be done by changing the width of the aerosol flow/inlet.

Figure 5b also shows a relatively large deviation of retrieved κ when D_d approaches 200 nm. This is due to the imperfect separation of the two hygroscopic modes by DMT-CCNC. As shown in Fig. 5a, the activation S drops as D_d increases. For $D_d \sim 200$ nm, a S of 0.37 % becomes so high that even aerosol particles in the less hygroscopic mode will be activated. This leads to an overestimate of activation fraction of the more hygroscopic mode and an underestimation of the corresponding κ.

The size-dependence of S suggests that a single S from DMT-CCNC will serve the separation purpose for a limited size range. To maintain the separation function, we need to adjust S according to the value of D_d. Figure S2 shows size dependent S for κ of 0.05. In practice, such scanning can be achieved by using a Scanning Flow CCN Analysis (SFCA) for DMT-CCNC.

3.3 Evaluation of BS2 approach

Figure 6 shows the experimental setup for evaluating the BS2 analysis. The setup is similar to normal size-resolved CCN measurements except that a nano-CCN counter (Wang et al., 2015) is used instead of a DMT-CCN counter. The nano-CCN counter was developed for measuring aerosol activation at the size range of 2 to 10 nm. In this size range, aerosol particles are of high diffusivity and go beyond the initial flow constraint. Thus aerosol particles are widely distributed in the activation unit of a nano-CCNC and BS2 analysis can be directly applied without modification of the system.

Figure 6 shows the F_{act}–$S_{aerosol}$ relation and F_{act}–κ relation determined from a size-resolved nano-CCNC measurement. The solid line represents the calibration curve (using tungsten oxides particles as calibration aerosol, Wang et al., 2015). It confirms the monotonic dependence of F_{act} on $S_{aerosol}$. Then by measuring F_{act} of mono-dispersed aerosols, we can determine $S_{aerosol}$ as well as κ (Eq. 2). As shown in Fig. 6, a larger F_{act} corresponds to a smaller $S_{aerosol}$ and a higher κ (more hygroscopic). Note that κ at this size range is different from previous CCN measurements due to the concentration and size dependence of κ and relevant thermodynamic parameters (Wang et al., 2015; Cheng et al., 2015).

Title Page

Abstract | Introduction

Conclusions | References

Tables | Figures

⏮ | ⏭

◀ | ▶

Back | Close

Full Screen / Esc

Printer-friendly Version

Interactive Discussion

4 Conclusions

As a new concept for the design of CCN counters, the broad supersaturation scanning (BS2) approach reduces the time required for scanning supersaturation and can produce κ of high temporal and size resolution. The principle of BS2 analysis has been demonstrated by laboratory experiments with a nano-CCNC. Model simulations show that the BS2 analysis is applicable for mixed particles with a single κ mode. It can also be applied to aerosol particles with multiple κ modes when complementary measurements are performed in parallel.

The BS2 approach requires relatively simple modification of existing thermal-gradient CCN counters (such as DMT-CCNC). The data process procedure of BS2 analysis is even easier than the present size-resolved CCN measurements. In addition, both temperature gradient and flow rate are kept constant during the measurements, minimizing the technical complexity and system stability. The fast response and stability of BS2 analysis are especially well suited for long-term measurements. Because κ is closely related to the fraction of organics/inorganics in aerosol particles, BS2 can also serve as a complementary sensor for fast detection/estimation of aerosol chemical compositions.

The Supplement related to this article is available online at doi:10.5194/amtd-8-9713-2015-supplement.

References

Cheng, Y., Su, H., Koop, T., Mikhailov, E., and Pöschl, U.: Size dependence of phase transitions in aerosol nanoparticles, Nat. Commun., 6, 5923, doi:10.1038/ncomms6923, 2015.

Fukuta, N. and Saxena, V. K.: A horizontal thermal gradient cloud condensation nucleus spectrometer, J. Appl. Meteorol., 18, 1352–1362, doi:10.1175/1520-0450(1979)018<1352:ahtgcc>2.0.co;2, 1979.

Gunthe, S. S., Rose, D., Su, H., Garland, R. M., Achtert, P., Nowak, A., Wiedensohler, A., Kuwata, M., Takegawa, N., Kondo, Y., Hu, M., Shao, M., Zhu, T., Andreae, M. O., and Pöschl, U.: Cloud condensation nuclei (CCN) from fresh and aged air pollution in the megacity region of Beijing, Atmos. Chem. Phys., 11, 11023–11039, doi:10.5194/acp-11-11023-2011, 2011.

Hudson, J. G.: An instantaneous CCN spectrometer, J. Atmos. Ocean. Tech., 6, 1055–1065, doi:10.1175/1520-0426(1989)006<1055:aics>2.0.co;2, 1989.

Köhler, H.: The nucleus in the growth of hygroscopic droplets, Trans. Faraday Soc., 32, 1152–1161, 1936.

Lance, S.: Quantifying compositional impacts of ambient aerosol on cloud droplet formation, PhD thesis, Georgia Institute of Technology, Atlanta, GA, USA, 2007.

Moore, R. H. and Nenes, A.: Scanning flow CCN analysis – a method for fast measurements of CCN spectra, Aerosol Sci. Tech., 43, 1192–1207, doi:10.1080/02786820903289780, 2009.

Petters, M. D. and Kreidenweis, S. M.: A single parameter representation of hygroscopic growth and cloud condensation nucleus activity, Atmos. Chem. Phys., 7, 1961–1971, doi:10.5194/acp-7-1961-2007, 2007.

Pruppacher, H. R. and Klett, J. D.: Microphysics of Clouds and Precipitation, Kluwer Academic Publishers, Dordrecht, the Netherlands, 1997.

Roberts, G. C. and Nenes, A.: A continuous-flow streamwise thermal-gradient CCN chamber for atmospheric measurements, Aerosol Sci. Tech., 39, 206–221, 2005.

Rose, D., Gunthe, S. S., Mikhailov, E., Frank, G. P., Dusek, U., Andreae, M. O., and Pöschl, U.: Calibration and measurement uncertainties of a continuous-flow cloud condensation nuclei counter (DMT-CCNC): CCN activation of ammonium sulfate and sodium chloride aerosol particles in theory and experiment, Atmos. Chem. Phys., 8, 1153–1179, doi:10.5194/acp-8-1153-2008, 2008.

Title Page

Abstract | Introduction

Conclusions | References

Tables | Figures

|◄ | ►|

◄ | ►

Back | Close

Full Screen / Esc

Printer-friendly Version

Interactive Discussion

Rose, D., Gunthe, S. S., Su, H., Garland, R. M., Yang, H., Berghof, M., Cheng, Y. F., Wehner, B., Achtert, P., Nowak, A., Wiedensohler, A., Takegawa, N., Kondo, Y., Hu, M., Zhang, Y., Andreae, M. O., and Pöschl, U.: Cloud condensation nuclei in polluted air and biomass burning smoke near the mega-city Guangzhou, China – Part 2: Size-resolved aerosol chemical composition, diurnal cycles, and externally mixed weakly CCN-active soot particles, Atmos. Chem. Phys., 11, 2817–2836, doi:10.5194/acp-11-2817-2011, 2011.

Su, H., Rose, D., Cheng, Y. F., Gunthe, S. S., Massling, A., Stock, M., Wiedensohler, A., Andreae, M. O., and Pöschl, U.: Hygroscopicity distribution concept for measurement data analysis and modeling of aerosol particle mixing state with regard to hygroscopic growth and CCN activation, Atmos. Chem. Phys., 10, 7489–7503, doi:10.5194/acp-10-7489-2010, 2010.

Wang, Z., Su, H., Wang, X., Ma, N., Wiedensohler, A., Pöschl, U., and Cheng, Y.: Scanning supersaturation condensation particle counter applied as a nano-CCN counter for size-resolved analysis of the hygroscopicity and chemical composition of nanoparticles, Atmos. Meas. Tech., 8, 2161–2172, doi:10.5194/amt-8-2161-2015, 2015.
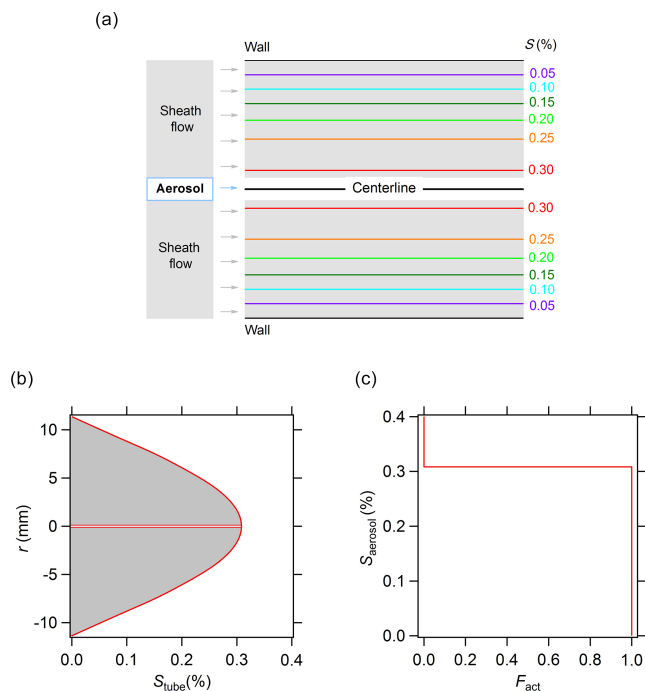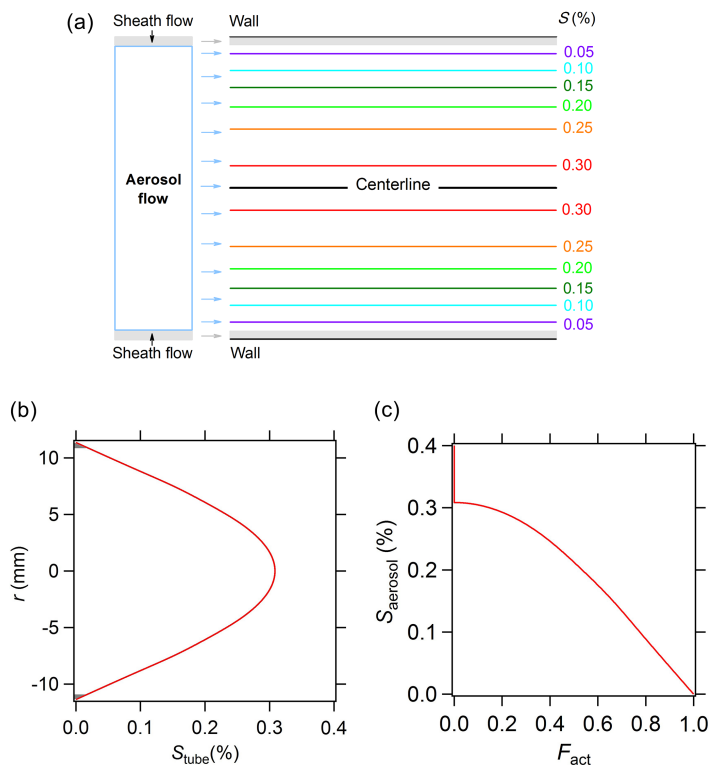
Figure 1. Schematics of typical CCN measurements. **(a)** Contour of supersaturation in the CCN activation unit and configuration of aerosol and sheath flow; **(b)** distribution of supersaturation in the activation unit (S_{tube}). r is the radial distance to the centerline. The shaded areas represent the sheath flow part and the non-shaded areas represent the aerosol flow part. The S_{tube} profile is adopted from http://nenes.eas.gatech.edu/Experiments/CFSTGC.html. **(c)** Plotting of the activation supersaturation of aerosol particles $S_{aerosol}$ against the activation fraction F_{act}.

Figure 2. Schematics of BS2-CCN measurements. **(a)** Contour of supersaturation in the CCN activation unit and configuration of aerosol and sheath flow; **(b)** distribution of supersaturation in the activation unit (S_{tube}). r is the radial distance to the centerline. The shaded areas represent the sheath flow part and the non-shaded areas represent the aerosol flow part. The S_{tube} profile is adopted from http://nenes.eas.gatech.edu/Experiments/CFSTGC.html. **(c)** Plotting of the activation supersaturation of aerosol particles $S_{aerosol}$ against the activation fraction F_{act}.

Figure 3. The activation fraction F_{act} measured by a BS2-CCNC as a function of particle dry diameter D_d and κ. S_{tube} profile of the BS2-CCNC is taken the same as in Fig. 2b.
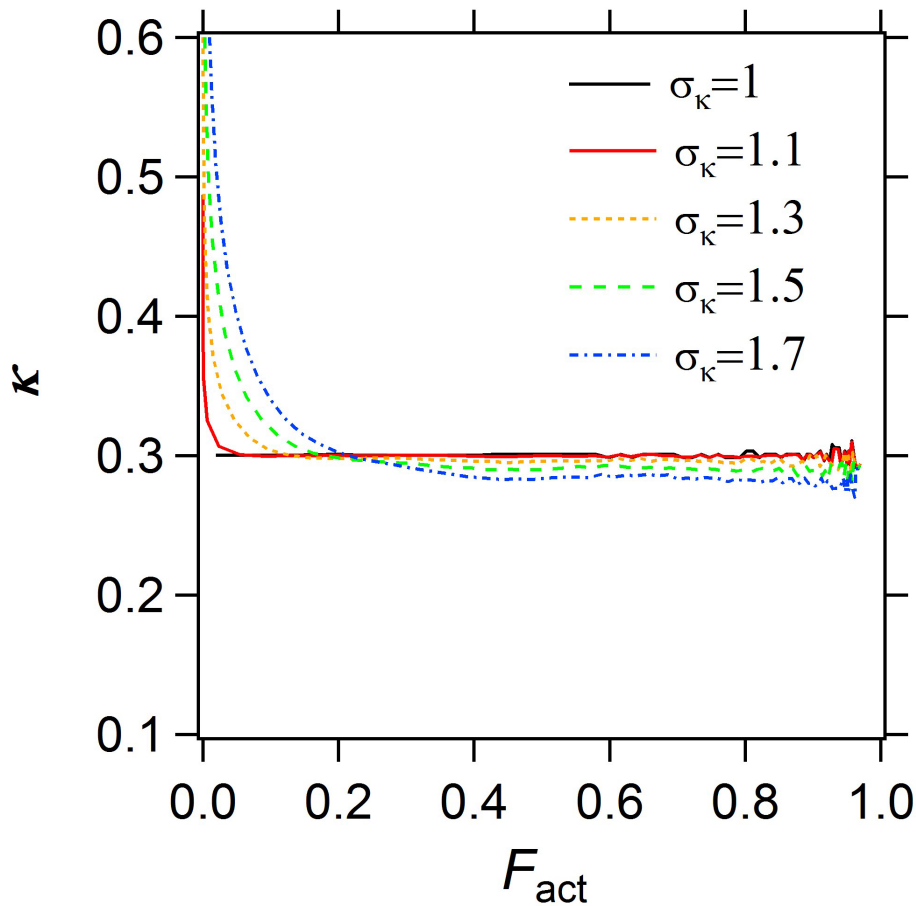
Figure 4. Influence of aerosol hygroscopicity (κ) distribution on the retrieval of κ by BS2-CCNC. σ_{κ} represent the geometric standard deviation of the aerosol hygroscopicity (κ) distribution.
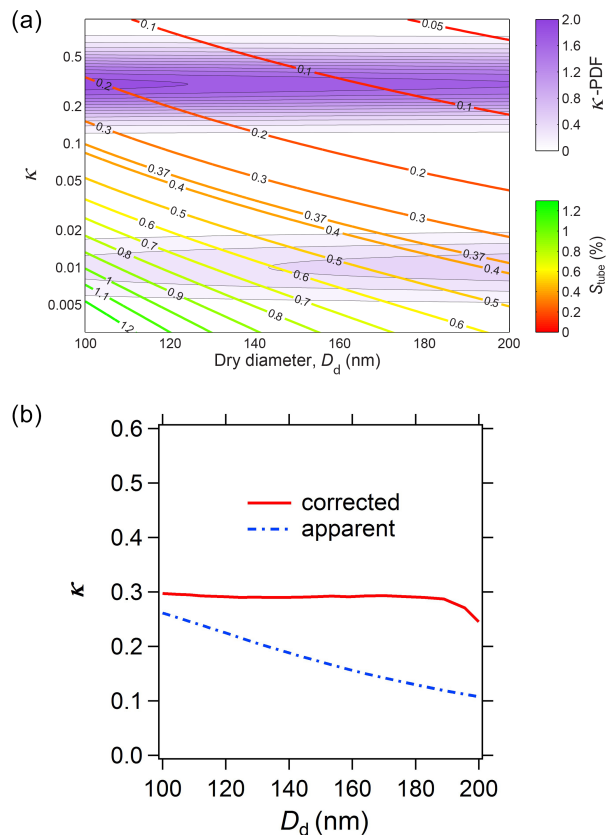
Figure 5. (a) Supersaturation required to activate the less hygroscopic mode by a DMT-CCNC. The shaded isolines describe the probability density function of a two-mode κ distribution. The colored isolines represent the supersaturation required to activate particles for certain dry diameter D_d and κ. **(b)** κ retrieved for the more hygroscopic mode by BS2-CCNC with (labeled as "corrected") and without (labeled as "apparent") complementary measurements of a DMT-CCNC.
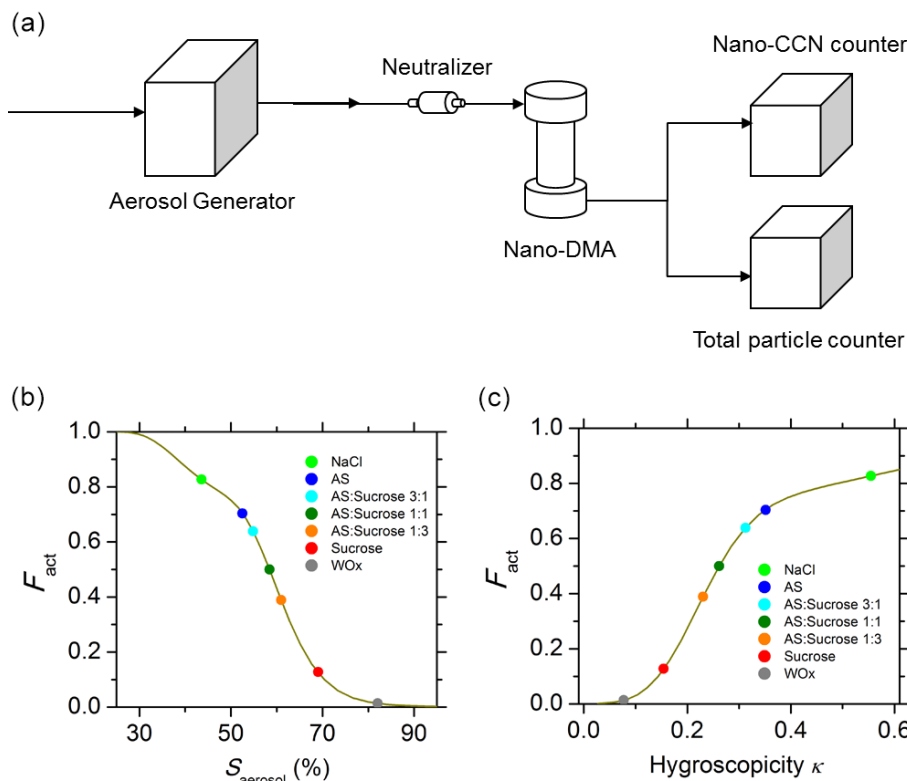
Full Screen / Esc

Figure 6. (a) Schematic of the setup for nano-CCNC measurements; **(b)** dependence of activation fraction F_{act} on the aerosol activation supersaturation $S_{aerosol}$ and **(c)** hygroscopicity κ for aerosols of dry diameter 2.5 nm. The solid line represents the calibration curve. The dots represent measurement results of different compounds in which AS denotes ammonium sulfate and WO$_x$ denotes tungsten oxides.